# Astro 358/Spring 2012

## Galaxies and the Universe

Figures + Tables for Lectures on Mar 20-27

---

## *Star Formation History of Galaxies: A Cornerstone of Galaxy Evolution*

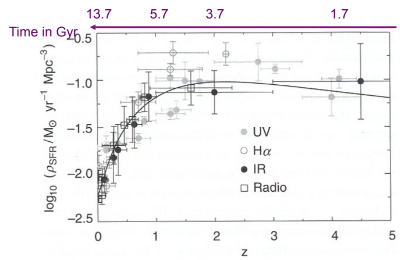


**Fig. 9.33.** The comoving star-formation density $\rho_{SFR}$ as a function of redshift, where the different symbols denote different indicators used for the determination of the star-formation rate. This plot, known as the "Madau diagram", shows the history of star formation in the Universe. Clearly visible is the decline for $z < 1$; towards higher redshifts,

(EAC)

---

## *Overview of how we measure Star Formation Rates*

---

The stellar Initial Mass Function (IMF)

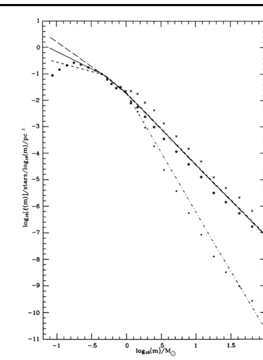


**Figure 22.** The stellar initial mass function (IMF) and present-day mass function (PDMF). The solid line represents the IMF given by equation (13), and the long- and short-dashed lines are for the cases $\alpha_1 = 1.85$ and 0.70, respectively. The PDMF ($\alpha_3 = 4.5$, Section 2) is indicated by the dot–dashed line. At masses below about 1 $M_\odot$ the PDMF equals the IMF. As a comparison, we show the PDMF derived by Scalo (1986) by solid dots. He corrects for stellar evolution; for a Galactic disc age of $T_0 = 9$ Gyr the IMF is indicated by stars, and for $T_0 = 12$ Gyr by crosses.

The solid line shows the stellar Initial Mass Function (IMF) from Kroupa (1993)

If we know the IMF, we can infer the star formation rate (SFR) from the massive SFR

## *3 important features of high mass stars*

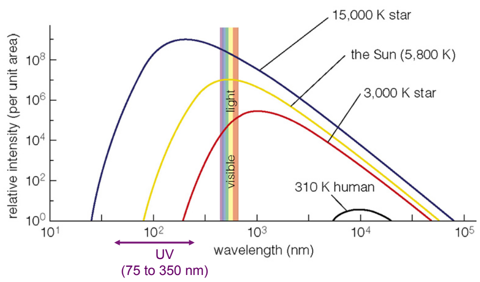


High mass (M>10 Mo, T>20,000 K) stars:

1) emit more ultraviolet light (750-3500 A or 75 to 350 nm) than low mass stars
2) emit Lyman continuum photons at $\lambda$<=912 A or 91.2 nm that ionize hydrogen
3) are short-lived (lifetime < $10^7$ yr for M>=10 $M_o$ star vs $10^{10}$ yr for 1 $M_o$ star)

## *Methods for estimating the Massive Star Formation Rate (MSFR)*

- MSFR from the UV continuum (750-3500 A)
- 
- MSFR from Ly continuum photons & Hydrogen Recombination Lines (Ly-alpha, Halpha, Pa-alpha, Br-gamma)

- MSFR from Thermal Radio continuum
- MSFR from Non Thermal Radio Continuum

- MSFR from Far-IR continuum
- MSFR from Mid-IR emission

## *MSFR from the UV light (750-3500 A) from massive stars*

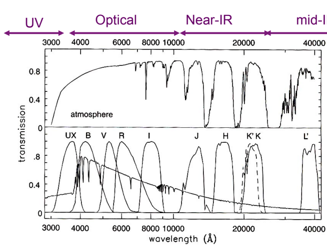


**Figure 1.7** Above, atmospheric transmission in the optical and near-infrared. Below, flux $F_\lambda$ of a model A0 star, with transmission curves $T(\lambda)$ for standard filters from Bessell, PASP 102, 1181; 1990. $UX$ is a version of the $U$ filter that takes account of atmospheric absorption. For $JHK'KL'$, $T(\lambda)$ is for transmission through the atmosphere and subsequently through the filter.

Credit:GU

1) Most of the UV light is absorbed by dust in the external galaxy, and re-radiated by warm dust at far-infrared ($4x10^5$ -$1.2x10^6$ A or 40-120 micron) wavelengths.
   → The far-infrared light is observed from space missions (Spitzer and Herschel) and provides a measure of the MSFR
2) The UV light, which is not absorbed by dust, is hard to observe
   → at $\lambda$ <=2800 A, the Earth's atmosphere blocks UV light (top figure): need space satellites like ASTRO-1 or GALEX
   → Over a narrow window ($\lambda$ =2800-3500 A) UV light can reach Earth telescopes

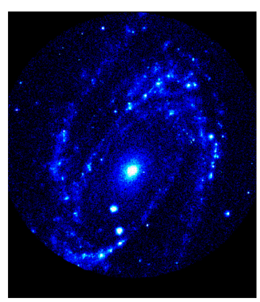

UV/ASTR0-1 image on M81
UV continuum ($\lambda$<3000 A) from high mass stars

Visible light image of M81

GALEX UV image of NGC 1291
UV continuum from high mass stars

Visible image of NGC 1291

## MSFR from UV light

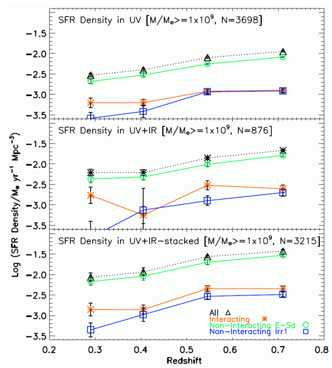


1) Top panel shows SFR_UV, the SFR derived from UV light.
This is calculated from ground-based images at 2800 A after doing extrapolations to cover the light emitted at $\lambda$=1216-3000 A, as well as at $\lambda$<1216 and $\lambda$>3000 A .

A Kroupa (2001) IMF is assumed

$SFR_{UV}$ = 9.8 x10-11 * 2.2 $L_{uv}$

$SFR_{total}$ = $SFR_{\_UV}$ + $SFR_{IR}$

(Jogee , Miller, Penne et al. & GEMS collaboratiion 2009, ApJ)

## Ly continuum photons from high mass stars ionize hydrogen

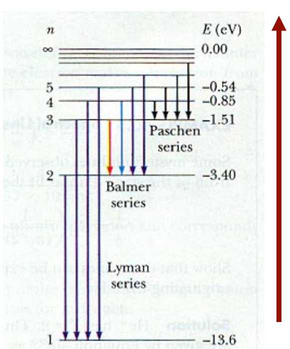


Ionization of H atom requires that it absorbs a Lyman continuum photon of $\lambda$ <= 912 A or Energy >=13.6 eV

## Ly cont photons disappear a few $10^7$yrs after the episode of SF

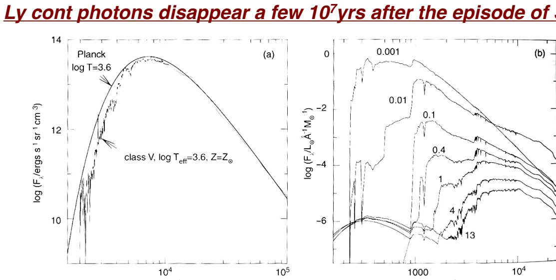


**Fig. 3.47.** **a)** Comparison of the spectrum of a main-sequence star with a blackbody spectrum of equal effective temperature. The opacity of the stellar atmosphere causes clear deviations from the Planck spectrum in the UV/optical. **b)** Spectrum of a stellar population with solar metallicity that was instantaneously born a time $t$ ago; $t$ is given in units of $10^9$ years

Right: For an episode of star formation that happened less than 0.01 Gyr or $10^7$ yrs ago, high M>10 Mo stars are still alive and produce Lyman continuum photons at $\lambda$<=912 A that ionize Hydrogen. As the stellar population ages beyond a few x$10^7$ yrs , the high mass stars die, and there are no Ly continuum photons

## *MSFR from Ly cont photons and Hydrogen Recombination lines*

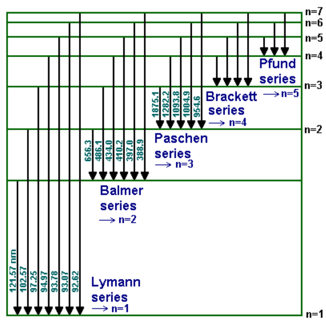


**Recombination lines of hydrogen**

**Emission** lines from electronic transitions from higher to lower levels:

- Lyman series ; UV
- Balmer series ; optical e.g H$\alpha$
- Paschen series; NIR
- Brackett series ; NIR
- etc

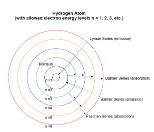

## *MSFR from Hydrogen H$\alpha$ Recombination lines*

**Purple = H$\alpha$ emission line**

Archetypal starburst galaxy M82. It shows the horizontal stellar disk of the galaxy, which harbors its active star formation, + a perpendicular supergalactic wind of ionized gas powered by the energy released in the starburst.

Credit: Mark Westmoquette (University College London), Jay Gallagher (University of Wisconsin-Madison), Linda Smith (Un. College London), WIYN//NSF, NASA/ESA

## *Tracing MSFR from UV and mid-infrared emission in M81*

UV/ASTR0-1
UV continuum from high mass stars

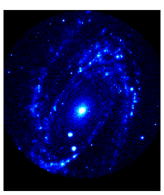

Visible light

Mid-IR/
Spitzer
at 24 mu =
hot dust
heated by
massive
young stars

NIR/Spitzer
3.6 mu
Underlying low mass stars

## *Tracing MSFR from mid to far-infrared emission*

Movie: From optical to IR view of M81 (Courtesy: NASA/Spitzer)

→ Near-IR at 1-3 micron: penetrates dust & shows low mass stars

→ Mid and far-IR from 10 to 100 micron shows **dust heated by massive young stars**

## Tracing MSFR from mid-infrared emission


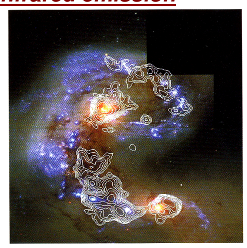

**Fig. 9.16.** The Antenna galaxies: superposed on the optical HST image are contours of infrared emission at 15 μm, measured by ISO. The strongest IR emission originates in optically dark regions. A large fraction of the star formation in this galaxy pair (and in other galaxies?) is not visible on optical images because it is hidden by dust absorption

(EAC)

Star formation is obscured at optical wavelengths by dust in gas-rich region, but revealed in **mid-infrared images that trace hot dust**

## Ultra Luminous Infrared Galaxies (ULIRGs)

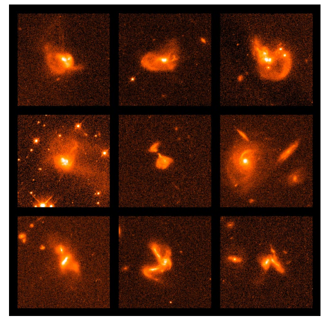

L_IR > 1e12 Lo → SFR > few 100 Mo yr-1
Most are strongly distorted systems: interactions/mergers

## MSFR from thermal + non-themal radio continuum

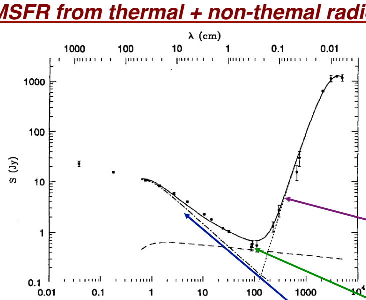


*Figure 1* The observed radio/FIR spectrum of M82 (Klein et al 1988, Carlstrom & Kronberg 1991) is the sum (*solid line*) of synchrotron (*dot-dash line*), free-free (*dashed line*), and dust (*dotted line*) components. The H II regions in this bright starburst galaxy start to become opaque below $\nu \sim 1$ GHz, reducing both the free-free and synchrotron flux densities. The free-free component is largest only in the poorly observed frequency range 30–200 GHz. Thermal reradiation from $T \sim 45$ K dust with opacity proportional to $\nu^{1.5}$ swamps the radio emission at higher frequencies. Lower abscissa: frequency (GHz). Upper abscissa: wavelength (cm). Ordinate: flux density (Jy).

Condon (1992)

Far-IR and radio spectrum of galaxies

The solid line is the total light and the 3 dashed lines show the contribution from 3 components:

- At short FIR wavelengths (0.01 cm or 100 microns) emission from warm 40 K dust dominate the spectrum
- Thermal free free radio emission dominates only over a narrow range of intermediate wavelengths
- At long wavelengths (20 cm) non-thermal radio continuum emission ( i.e., synchrotron emission) dominate spectrum

## (SFR from UV and Hα) vs (SFR from Far-IR and radio)

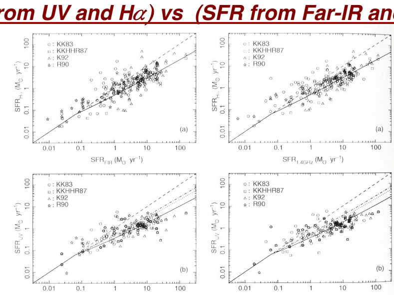


**Fig. 9.32.** Correlations of the star-formation rates in a sample of galaxies, as derived from observation in different wavebands. In all four diagrams, the dashed line marks the identity relation $SFR_i = SFR_2$; as is clearly seen, using the Hα luminosity and UV radiation as star-formation indicators seems to underestimate the SFR. Since radiation may be absorbed by dust at these wavelengths, and also since the amount of warm dust probably depends on the SFR itself, this effect can be corrected for, as shown by the solid curves in the four panels

EAC

SFR estimates based on UV continuum or optical Hα recombination line
→ are affected and dust and can under-estimate the SFR
→ are typically < SFR estimates from longer wavelength tracers (Far-IR or radio continuum) which are less affected by dust

## *Conditions for the Onset of Star Formation*

## *Collapse of a molecular cloud to form stars*

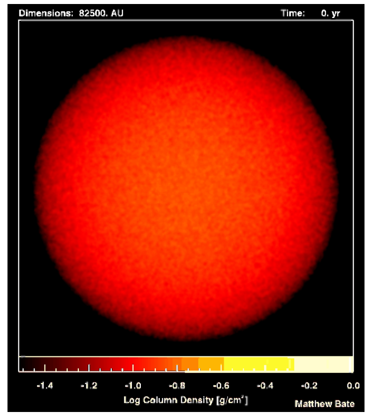


The simulation shows the collapse and fragmentation a molecular cloud of mass 50 Mo, with initial diameter of ~0.4 pc , temperature of 10 K.

→ Jean mass $M_J$ = 1 Mo for T=10 K, n=$10^5$ atoms cm-3

High density regions within the cloud gravitationally collapse and fragment to form stars

Surrounding some of these stars are swirling discs of gas which may go on later to form planetary systems like our own Solar System.

## *Evidence for suppression of SF at large radii in disk of spirals*

Kennicutt 1989

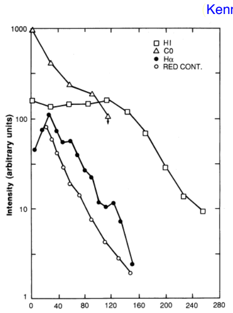


FIG. 4.—Radial profiles of H I, CO, Hα, and red continuum surface brightness in NGC 4254. Data are plotted on a relative scale, but the H I and CO profiles are normalized to a common surface density scale. The truncation of the Hα profile at a radius of 150″ is real.

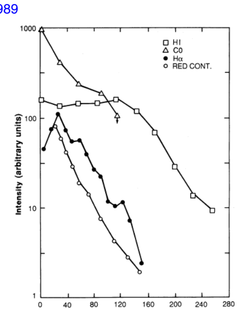


FIG. 4.—Radial profiles of H I, CO, Hα, and red continuum surface brightness in NGC 4254. Data are plotted on a relative scale, but the H I and CO profiles are normalized to a common surface density scale. The truncation of the Hα profile at a radius of 150″ is real.

SFR traced by Hα appears suppressed at large radii although atomic hydrogen (HI) is present

## *Evdence of a threshold gas density for SF in disk of spirals*

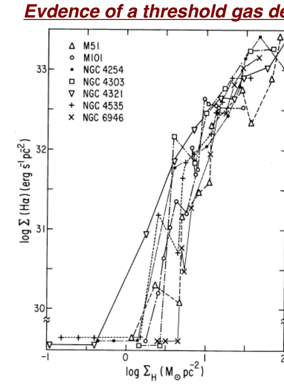


FIG. 8.—Dependence of Hα surface brightness on total (H I + $H_2$) hydrogen surface density, for seven giant Sc galaxies. Each point represents the Hα and gas densities averaged at a given galactocentric radius, and lines connect points at adjacent radii. The points at the bottom denote regions where no Hα emission was detected.

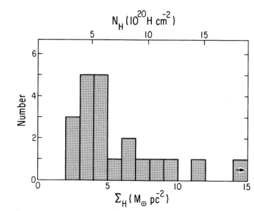


FIG. 9.—Distribution of threshold column densities in the sample. The bottom scale is in units of total (H I + $H_2$) hydrogen mass surface density, and the top scale is in units of hydrogen column density.

Kennicutt 1989

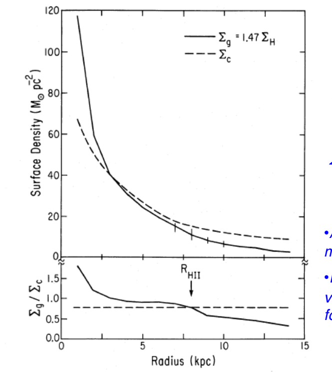


FIG. 10.—Top panel shows the radial distribution of total (atomic and molecular) gas surface density in NGC 6946 (*solid line*), and the radial dependence of the threshold surface density for gravitational stability, from eq. (4). Bottom panel shows the radial dependence of the ratio of these two densities. The vertical arrow denotes the radius of the H II region disk, and the horizontal dashed line indicates the value of $\Sigma_g/\Sigma_c$ at this radius.

*Using the gravitational instability model to account for the threshold gas density for SF disk of spirals*

$$\Sigma_{crit} = \alpha\ (\kappa\,\sigma/3.36\,G\Sigma) = \alpha\,\Sigma_c$$

- *At each radius R calculate $\Sigma_c$ and measure total gas density $\Sigma_g$*
- *Plot $(\Sigma_g/\Sigma_c)$ vs radius R: its value at the threshold radius $R=R_{HII}$ for star formation gives $\alpha$*

Kennicutt 1989

*Using the gravitational instability model to account for the threshold gas density for SF disk of spirals*

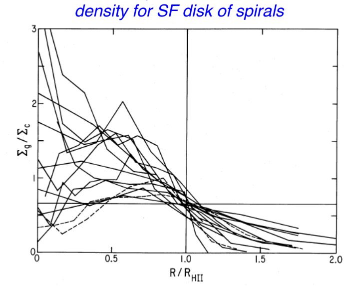


FIG. 11.—Radial dependence of the ratio of gas surface density to the critical density for gravitational stability (eq. [4]), for the galaxies with active star-forming disks. The radial coordinate is normalized to the radius of the H II region disk. The horizontal line indicates the value for the stability parameter ($\alpha$ = 0.67) which best fits the observed star formation thresholds. Dashed lines denote M33 and NGC 2403.

$$\Sigma_{crit} = \alpha\ (\kappa\,\sigma/3.36\,G\Sigma) = \alpha\ \Sigma_c$$

*$\alpha \sim 0.7$ for all galaxies !*

Kennicutt 1989

## *Schmidt Law relating $\Sigma$gas and $\Sigma$sfr*

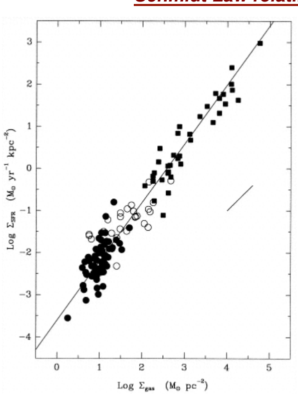


(Kennicutt 1998)

***$\Sigma_{SFR}$ prop to $(\Sigma_{gas})^n$***

Composite star formation law for the normal disk (filled circles) and starburst (squares) samples.

Open circles show the SFRs and gas densities for the centers of the normal disk galaxies.

The line is a least-squares fit with index N = 1.40. The short diagonal line shows the effect of changing the scaling radius by a factor of 2.

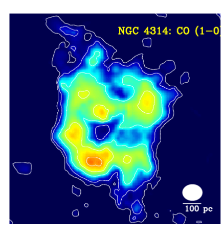


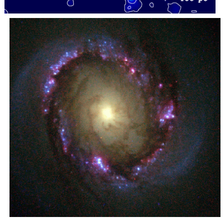

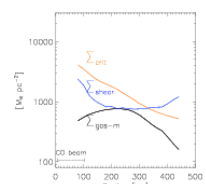


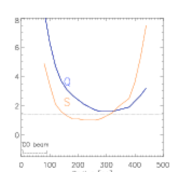


## *SF in the central kpc*

In the central kpc of NGC 4314, the Toomre Q parameter is a minimum (~1-2) in regions of SF and rises sharply insde the ring of SF.

Is there a critical density for SF in the inner kpc controlled by gravitational instabilities?

(Jogee, Scoville & Kenney 2005)

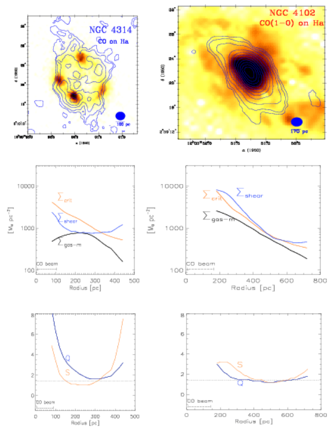


## *SF in the central kpc*

In the central kpc of both NGC 4314 and NGC 4102 the Toomre Q parameter is a minimum (~1-2) in regions of SF

(Jogee, Scoville & Kenney 2005)

## *Feedback on Star Formation (stellar and AGN)*

## *Stellar Feedback on Star Formation*

Massive stars formed in a recent star formation episode can exert "feedback" to suppress the very star-formation process that produced them (no good deed goes unpunished! )

The feedback happens via supernovae and winds associated with the massive stars in different ways, e.g.,

1) Energy or momentum from supernovae and winds can be transferred to the ambient gas, which is blown out to large scale heights in a starburst wind. (The ejected gas can escape if its speed > escape speed at relevant radii or later rain back on the galaxy)

2) Cold atomic (and molecular) gas fueling star formation can be heated by shocks, plus it can be dynamically heated (its velocity dispersion rises). This makes the gas less susceptible to gravitational instabilities, such as those believed to convert atomic gas into molecular hydrogen.

## *Feedback on SF frrom SNe driven winds*

Purple = Ha emission line

Starburst galaxy M82.

Note perpendicular starburst wind of ionized gas powered by the energy released in the starburst.

Credit: Mark Westmoquette (University College London), Jay Gallagher (University of Wisconsin-Madison), Linda Smith (Un. College London), WIYN//NSF, NASA/ESA

## Feedback from Active Black holes

## Feedback on SF from Black Holes

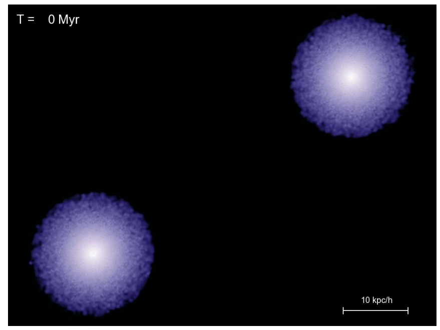


Di Matteo et al 2005
This computer animation visualizes the time evolution of a merger simulation of two spiral galaxies that host supermassive black holes at their centres. Only the gas distribution is shown. Brightness represents gas density, whereas the colour hue indicates gas temperature.

## Outstanding Questions

## What drives decline in cosmic SFR density over z =1 to 0

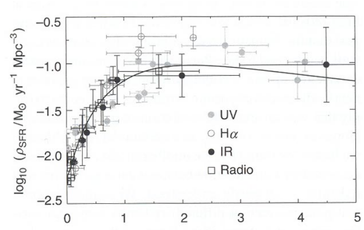


Decline in frequency of galaxy mergers and interactions
Decline in cold gas content due to gas consumption/removal by SF/AGN
Decline in accretion rate from filaments
Transition of SF to lower mass

## *Example of interacting/merging galaxies at lookback =3 to 8 Gyr*




## *Example of interacting/merging galaxies at lookback =3 to 8 Gyr*

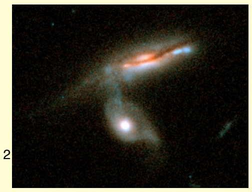
2


## *SFR density from mergers over last 7 Gyr*

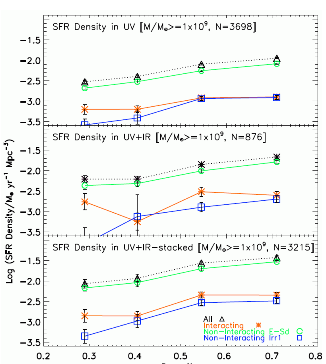


For M*>=1e9 Mo & M*>=2.5e10 visible mergers account for less than 30% of the SFR density over the last 7 Gyr. Most (above 70%) of the SFR density comes frrom normal non-interacting systems !!

**Implications**

1) the behavior of the SFR density over the last 7 Gyr is shaped by non-interacting galaxies rather than mergers,

2) At half of its present age, the Universe had already transitioned from a violent to a fairly quiescent phase and the evolution of massive galaxies was no longer dominated by mergers

(Jogee, Miller, Penne, et al. & GEMS collaboratiion 2009, ApJ)